

Preclinical Development and Evaluation of Allogeneic CAR T Cells Targeting CD70 for the Treatment of Renal Cell Carcinoma

Authors

Siler H. Panowski¹, Surabhi Srinivasan¹, Nguyen Tan¹, Silvia K. Tacheva-Grigorova¹, Bryan Smith¹, Yvonne S.L. Mak¹, Hongxiu Ning¹, Jonathan Villanueva¹, Dinali Wijewarnasuriya¹, Shanshan Lang¹, Zea Melton¹, Adit Ghosh¹, Mathilde Dusseaux⁴, Roman Galetto⁴, Jonathan R. Heyen³, Tao Sai², Thomas Van Blarcom¹, Javier Chaparro-Riggers², and Barbra J. Sasu¹

Affiliations

¹ Allogene Therapeutics, South San Francisco, California

² Pfizer Worldwide Research and Development, South San Francisco, California

³ Drug Safety Research and Development, Pfizer Worldwide Research and Development, La Jolla, California

⁴ Cellectis, Paris, France

Note: Siler Panowski and Surabhi Srinivasan contributed equally to this work.

Corresponding Authors: Siler Panowski, Allogene Therapeutics, Inc. 210 East Grand Avenue, South San Francisco, CA 94080. Phone: 650-615-7555; Email: siler.panowski@allogene; and Barbra Sasu, Allogene Therapeutics, Inc. 210 East Grand Avenue, South San Francisco, CA 94080. Phone: 650-826-5114; Email: barbra.sasu@allogene.com

Running Title Preclinical Development of Allogeneic CD70 CAR T Cells

Conflict of interest disclosure statement: All authors are current or former employees of Pfizer Inc., Allogene Therapeutics, or Cellectis.

Significance: These findings demonstrate the efficacy and safety of fratricide-resistant, allogeneic anti-CD70 CAR T cells targeting renal cell carcinoma and the impact of CAR epitope on functional activity.

Abstract

CD70 is highly expressed in renal cell carcinoma (RCC), with limited expression in normal tissue, making it an attractive CAR T target for an immunogenic solid tumor indication. Here we generated and characterized a panel of anti-CD70 scFv-based CAR T cells. Despite the expression of CD70 on T cells, production of CAR T from a subset of scFvs with potent *in vitro* activity was achieved. Expression of CD70 CARs masked CD70 detection in cis and provide protection from CD70 CAR T-mediated fratricide. Two distinct classes of CAR T cells were identified with differing memory phenotype, activation status, and cytotoxic activity. Epitope mapping revealed that the two classes of CARs bind unique regions of CD70. CD70 CAR T cells displayed robust antitumor activity against RCC cell lines and patient-derived xenograft mouse models. Tissue cross-reactivity studies identified membrane staining in lymphocytes, thus matching the known expression pattern of CD70. In a cynomolgus monkey CD3-CD70 bispecific toxicity study, expected findings related to T cell activation and elimination of CD70-expressing cells were observed, including cytokine release and loss of cellularity in lymphoid tissues. Lastly, highly functional CD70 allogeneic CAR T cells were produced at large scale through elimination of the T cell receptor by TALEN-based gene editing. Taken together, these efficacy and safety data support the evaluation of CD70 CAR T cells for the treatment of RCC and has led to the advancement of an allogeneic CD70 CAR T candidate into phase I clinical trials.

INTRODUCTION

Renal cell carcinoma (RCC) is an area of high unmet need and represents a substantial patient population, with 74,000 new cases and 15,000 deaths estimated in the US each year (1). New therapies for RCC, including PD-1-targeting agents and combinations, show promising initial response, but low CR (complete remission) rates of 6-16%, highlighting the need for additional treatment options (1-6).

RCC is a highly T cell infiltrated tumor type and thus may be amenable to a T cell-based therapy (2-4,7). Adoptive transfer of T cells expressing chimeric antigen receptors (CARs) is a promising therapy showing substantial benefit in hematologic malignancies, including the recent approval of CD19- and BCMA-targeting CAR T therapies (8-10). Approved CAR T therapies are based on use of a patient's own T cells (autologous). While highly effective in the clinic, this approach has challenges, including significant time for production and variability in performance of patient-derived cells (11,12). Allogeneic CAR T cell therapy, or "off-the-shelf" therapy is a next-generation CAR T modality that utilizes cells from healthy donors and may overcome many of these challenges by increasing both the number of patients treated and product activity and consistency (13-20).

Allogeneic CAR T cells can be created by TALEN® gene-editing at the TRAC loci to avoid graft versus host disease (GvHD) and the CD52 loci to confer resistance to ALLO-647, an anti-CD52 antibody used as part of the conditioning regimen to extending the window of T cell engraftment (21).

To translate this approach for RCC treatment, public expression data were mined to identify targets with a high prevalence in RCC and low/absent expression in normal tissues. *CD70* was identified as a gene expressed in a high proportion of patients with RCC and has limited normal tissue expression in a small subset of activated lymphocytes, stromal cells of the

thymic medulla, and antigen presenting cell (APCs) (22-24). CD70 is the ligand for the T cell co-stimulatory receptor CD27, activation of which generally leads to increased T cell persistence and memory formation (25,26). *CD70* is also aberrantly expressed at high levels in a variety of hematological malignancies and solid tumors (27,28). The role of CD70 in cancer is only partially elucidated. CD70 is thought to play an immunosuppressive role in solid tumors by possibly overstimulating CD27 in the absence of productive co-stimulation, leading to T cell apoptosis and immune escape (29,30).

Previous studies have reported the use of truncated CD27-based CARs to target CD70 (30-32). This study is the first to demonstrate *in vitro* and *in vivo* analysis of multiple single chain fragment variable (scFv)-based anti-CD70 CAR T cell clones and identify a potential clinical product. Despite expression of CD70 on activated T cells, CAR T generation was successful, and cells did not succumb to mass fratricide. Avoidance of fratricide may be due to cis masking of CD70 by CAR expression. Several selected candidates were tested for appropriate specificity in tissue-cross-reactivity assays and one candidate was shown to have an acceptable toxicity profile in a cynomolgus monkey study when formatted as a CD70/CD3 bispecific. Allogeneic CD70 CAR T cells were generated from healthy donor T cells and manufactured successfully in a large-scale process allowing for the treatment of many patients with a single run.

The impressive preclinical efficacy and safety data of the lead candidate CD70 CAR T cells presented in this manuscript and the promise of next-generation allogeneic CAR T cell therapy support the clinical investigation of allogeneic CD70 CAR T cell for the treatment RCC.

MATERIALS AND METHODS

Cell lines

786-O (CRL-1932), ACHN (CRL-1611), REH (CRL-8286), HEK293T (CRL-3216), and Jurkat (TB-152) cell lines were acquired from ATCC. No authentication was performed, and all cells were purchased directly from the source. Early passages of cells were frozen down and prior to initiating experiments cells were thawed and passaged 2-3 times. No misidentified cell lines were used. All cell lines were tested for mycoplasma and were negative.

Staining and quantification of CD70 by flow cytometry

Cells were stained with 1 or 10 $\mu\text{g/mL}$ PE-conjugated clone 41D12, generated at Allogene based on published sequences (33). Antibody binding capacity was quantified using Quantibrite PE beads (BD Biosciences) following manufacturer's protocol. Samples were acquired on CytoFLEX flow cytometer (Beckman Coulter).

CAR characterization in Jurkat and primary T cells

Jurkat cells or primary T cells were transduced with CAR-containing lentiviral vector (LVV) as described in Supplemental Methods. Activation (CD69) was determined four days post-transfection by flow cytometry. TRAC, CD52, or CD70 were edited on Day 6 by electroporation with TALEN® mRNA (Collectis & TriLink Biotechnologies). Cells were stained on Day 9 with anti-CD70, anti-CD25, and anti-4-1BB, and on Day 14 with anti-CD62L and anti-CD45RO. Recombinant human IL-2 was added throughout T cell culture and TCR $\alpha\beta$ -positive cells were depleted using TCR $\alpha\beta$ isolation kit (Miltenyi Biotec) at the end of process. T cells were cryopreserved in 90% FBS/10% DMSO.

***In vitro* cytotoxicity assays**

Luciferase-expressing 786-O, ACHN, and REH target cells were co-cultured with CAR⁺ T cells at defined E:T ratios for 72 hours. Target viability was determined by ONE-Glo reagent (Promega). For long-term serial killing assays, target cells and CAR T cells were co-cultured as described above. Every three- or four-days cells were mixed and half the T cells were transferred to a new plate of target cells. Target cell viability in the spent plate was read out by ONE-Glo reagent. Additional details are provided in Supplemental Methods.

CD70 masking and protection assays

Luciferase-expressing ACHN cells were transduced with CAR LVVs and stained with CAR Fabs at 2.5 µg/mL followed by anti-His antibody at 1:50 dilution. CAR-expressing ACHN cells were subjected cytotoxicity assays as described above.

RCC xenograft models

All animal studies were performed under approval by the Allogene Therapeutics Institutional Animal Care and Use Committee (IACUC). 786-O cells were implanted subcutaneously with Matrigel at 5×10^6 cells/mouse. Tumors were measured twice weekly using calipers. ACHN-nucLucGFP cells were injected IV at 1×10^6 cells/mouse. Bioluminescence measurements were performed twice weekly using the IVIS Spectrum. NSG mice bearing patient derived RCC xenograft tumors were purchased from Jackson Laboratory. Tumor volume was measured twice weekly by calipers. CAR T cells generated as previously described were thawed and dosed via IV injection. Animals were euthanized when they exhibited disease model-specific endpoints. Additional details are provided in Supplemental Methods.

Normal kidney staining and cytotoxicity

Fresh kidney tissues dissected into cortex and medulla (Biobank Online) were dissociated using multi-tissue dissociation kit 1 (Miltenyi). Cells were stained with CAR 23 or isotype scFv-Fc protein followed by anti-Fc-PE antibody. Dissociated kidney and CAR 23 cells were co-cultured at a 1:1 ratio for 24 hours in RPMI1640 plus 10% FBS. Cells were stained with anti-CD69 antibody and viability dye before acquisition.

Cynomolgus monkey study

CAR 23 and CD3 antibodies were reformatted into a bispecific antibody. Two cynomolgus monkeys (one male and one female), ~3 years old at initiation of dosing, were administered the bispecific at 30 µg/kg by IV injection on Day 1. On Day 8 the same animals were administered a dose of 100 µg/kg. Vehicle (PBS) was administered to the control group. Clinical observations, body weight measurements, qualitative food consumption, and body temperature measurements were collected prior to initiation of dosing (PID) and at additional specific timepoints. Samples were collected for hematology, coagulation, clinical chemistry, immunophenotyping, and cytokine analysis PID and/or at additional specific timepoints. Cytokine analysis was performed using the Milliplex MAP Non-Human Primate Cytokine Magnetic Bead Panel (Millipore). Necropsy was performed at the end of the study for microscopic and macroscopic examination of tissues.

Statistical analysis

All statistics were performed in GraphPad Prism 8. Animal tumor volume or flux (log transformed) was matched into groups with equal means and variance. Each group was then randomly assigned a treatment. Average mean tumor volume or bioluminescence was analyzed

for all mice and statistics were performed on replicate measurements from the day of CAR T dosing until the day the animals in the control group were euthanized. For statistical analysis, tumor growth in the treatment groups was compared against the control group, using repeated-measures (RM) one-way analysis of variance (ANOVA) with either Dunnett's or Tukey's multiple comparison test. Gaussian distribution and sphericity were assumed.

Data availability statement

All data associated with this study are presented in the paper or Supplemental Material. Reagents can be provided by and at Allogene's sole discretion pending scientific review and completion of a material transfer agreement with Allogene.

RESULTS

CD70 expression on renal cell carcinoma cell lines and tumors

To identify suitable RCC tumor associated antigens (TAAs), RNA expression data from the TCGA and GTEX databases were analyzed. *CD70* was found to be highly expressed in RCC and had minimal expression in normal tissues (Fig. 1A). *CD70* RNA in RCC tumors displayed median expression slightly lower than that observed in ACHN cells and a maximum equivalent to 786-O cells (Fig. 1B). *CD70* protein staining by IHC was localized to the cytoplasm and cell membrane, with strong/moderate staining in 69% of clear cell RCC (ccRCC; Fig. 1C and D). *CD70* cell-surface protein expression as determined by flow cytometry was observed on RCC

cell lines and primary patient samples (Fig.1E) with a median receptor density in patient samples of 7k/cell (Figure 1F). Expression was also evaluated on T cells and was observed on activated but not resting cells (Fig 1G).

Unique classes of CD70 CAR T cells with distinct behaviors and cytolytic activity

Phage display and hybridoma anti-CD70 antibody generation was performed (34,35). Forty-six antibodies were selected based on binding and specificity by ELISA and flow cytometry. These antibodies were formatted into second generation 4-1BB CARs and screened to eliminate clones exhibiting autoactivation (target-independent CAR aggregation) (36). CD70 wildtype and CD70 knockout (KO) Jurkat cells transduced with CARs were used and activation in the absence of target was monitored. Eight strongly auto-activating CARs displayed high CD69 in the absence of target (CD70 KO Jurkats) and were removed from further evaluation (Fig. 2A).

CARs were next transduced into primary T cells using lentiviral vectors. The majority of clones (92%) displayed transduction efficiency greater than 25% (Fig. 2B) and expansion of over 50-fold. Evaluation of CD70 expression on CAR T cells revealed two general classes of CARs: those with minimal CD70 detection using an anti-CD70 FACS detection reagent: termed class 1, and those with clear CD70 detection: termed class 2 (Fig 2C). Twelve class 1 CARs and eleven class 2 CARs were characterized further and revealed that class 1 CAR T cells are more differentiated and had a higher basal activation status (4-1BB/CD25 double positive), as compared to class 2 CARs (Fig. 2D-E, Supplementary Table S1).

To evaluate CAR functionality a 3-day cytotoxicity assay was performed against cell lines with a range of CD70 expression. In general, class 1 CARs were highly effective and lysed target cells across the CD70 expression range, whereas only three class 2 CARs displayed target lysis >50% (Fig 2F, Supplementary Fig S1, Supplementary Table S1). Overall, CARs with lower

levels of CD70 detection at the end of culture (<5%) had the greatest short-term cytotoxic potential/activity (Fig. 2G).

A long-term serial-killing assay was developed to evaluate CAR susceptibility to exhaustion following repeated target exposure. All CARs were able to kill target cells initially, but many lost activity after repeated re-challenge. Class 1 CARs performed well against all target cells. Class 2 CAR were highly active against CD70-high targets but performed poorly when CD70 expression was low (Fig. 2H).

CD70 CAR expression protects CAR T cells from fratricide

The relationship between CD70 detection and cytotoxic activity (Fig. 2G) prompted experiments to better understand the differences between class 1 and 2 CARs and to determine if lack of CD70 detection on class 1 CAR T cells is due to the killing of CD70⁺ cells in culture (fratricide) or prevention of detection through cis masking of CD70 by the CAR, obscuring the detection epitope (Fig. 3A). Jurkat cells were used because they are a CD4-derived cell line incapable of cytotoxicity and fratricide. CD70 detection on CAR Jurkat cells mirrored what was seen for primary CAR T cells, with the same subset of CARs being CD70 negative, thus the lack of CD70 detection must be due to masking (Fig. 3B and C).

Next, affinities of clones were examined. The binding domains of CARs were reformatted as Fabs (since not all CARs could be expressed as soluble scFvs). Affinities for recombinant human CD70 protein ranged between 0.15nM-19nM for class 1 CARs and 1.4nM-47nM for class 2 CARs as determined by biosensor assays (Supplementary Fig. S2). No clear trend in affinity and CD70 detection or CAR T activity was observed.

CAR Fabs were also subjected to binning and epitope mapping. The two classes of CARs fit largely into two distinct bins. An outlier was CAR 24, which did not co-bind with any of the

other Fabs and was designated subclass 2b (Supplementary Fig. S2). To perform epitope mapping, point mutations of CD70 residues were generated and key residues to binding of each CAR Fab identified. All class 1 CARs targeted epitopes ranging from the apex to the side of CD70, while class 2 CARs targeted epitopes located at the bottom of CD70 (Fig. 3D, Supplementary Fig. S3).

Experiments were carried out to demonstrate the ability of cis masking to obscure CD70 detection. ACHN or T cells transduced with or without CARs were stained for CD70 with either class 1 or class 2 Fabs (Fig. 3E, Supplementary Fig. S4A-B). Class 1 Fabs were unable to stain cells expressing class 1 CARs but were able to stain cells expressing class 2 CARs and vice versa. The exception to this observation was the inability of any of the Fabs to stain cells expressing CAR 23, suggesting this CAR may have unique properties and fall into a subclass (designated 1b). CD70 was not detected on any cells by the CAR 24 Fab, potentially because this Fab has a fast dissociation rate (Supplementary Fig. S2).

To examine biological consequences of masking, ACHN cells expressing the various CARs were subjected to cytotoxicity assays with primary CD70 CAR T cells. Expression of class 1 CARs by target cells was able to protect against lysis by class 1 CAR T cells, but not class 2 CAR T cells (Fig. 3F). The inverse was true for class 2 CARs (Fig. 3G). Despite the ability of CAR 23 to prevent detection by both class 1 and class 2 Fabs (Fig. 3E), it was only susceptible to killing by class 2 CAR T cells. CAR 24 continued to stand apart from other class 2 CARs in that it was only able to protect against killing by itself.

Effects of CD70 knockout (KO) on CAR T cell activity *in vitro* and *in vivo*

Despite the potential protective effects of cis masking in CD70 CAR T cells, interaction of CAR and untransduced CD70⁺ T cells in culture may still lead to overactivation and exhaustion. For

this reason, CD70 KO was evaluated in two CAR clones to determine if functional activity could be further improved. CD70 KO using TALEN® gene editing successfully eliminated CD70 expression on T cells at the end of culture (Fig. 4A). CD70 KO did not alter CAR T expansion/yield or cytotoxic activity *in vitro* as compared to the non-gene edited cells (Fig. 4B; Supplementary Fig. S5). To better evaluate the effects of CD70 KO on CAR T activity, two *in vivo* RCC xenograft models, a subcutaneous model with very high CD70 expression, 786-O, and a metastatic disease model with levels more similar to RCC patients, ACHN, were developed. Dose response studies were performed with both models using CAR 23. In both studies a clear dose response was observed and 3×10^6 was selected as a suboptimal dose for efficacy comparison (Fig. 4C&D). In a 786-O study to evaluate CAR 23 and CAR 24 activity with and without CD70 KO, CAR 24 showed superior activity and complete tumor eradication and CAR 23 showed partial tumor eradication (Fig. 4E). Knockout of CD70 in the CAR T cells did not alter activity of CAR 24, but did improve the functionality of CAR 23. CD70 KO was next evaluated in the ACHN model at the same dose. CAR 23 was superior to CAR 24 in this model. CD70 KO had no significant effect on the activity of either CAR (Fig. 4F). CAR 24 and similar CARs that displayed sub-optimal activity against lower CD70-expressing cells *in vitro* (Fig. 2H) were eliminated from further evaluation.

CD70 CAR T with rituximab-based off-switches

A CAR off-switch may be desired to eliminate CAR T cells in the case of unexpected adverse activity (37,38). A rituximab-based off-switch system was selected, as rituximab is a widely used anti-CD20 antibody and such a system can effectively modulate CAR activity (38-40). Three rituximab formats (R-formats) were evaluated with varying mimotope number and location (Fig. 5A). The top five performing CARs from the long-term *in vitro* cytotoxicity studies (Fig. 2H)

were converted into R-formats and transduced in primary T cells. All R-format CAR T cells with transduction above 40% (Fig. 5B; Supplementary Fig. S6A) were tested in cytotoxicity assays and were able to eliminate target cells effectively, although some differences in activity between formats were observed (Fig. 5C&D). Optimal R-format CARs were generally equal or better than their “naked” CAR counterparts and this was particularly true for CAR 23, which was significantly more effective both *in vitro* and *in vivo* in the QR3 format as compared to the “naked” CAR (Fig. 5E; Supplementary Fig. S6B). R-format off-switch functionality upon addition of rituximab was tested in ADCC *in vitro* assays and significant depletion of CAR T cells was observed (Supplementary Fig. S6C).

CAR T clones in optimal R-formats based on CAR expression and cytotoxic activity were moved into *in vivo* studies. In the CD70-high 786-O model, a dose of 5×10^6 CAR T cells per animal resulted in early tumor regression for all CARs and durable responses for CARs 3, 17, and 23 (Fig. 5F). Peak CAR 23 QR3 T cell expansion occurred between day 13 and day 21 and cells were able to reject a tumor rechallenge on day 24 (Supplementary Fig. S7A-E). A similar ranking held true in an ACHN tumor study, with durable responses out to 90 days in some cases (Fig. 5G; Supplementary Fig S7F-G). *In vivo* functionality in a highly relevant subcutaneous PDX study was evaluated utilizing CARs 17 and 23. Despite relatively low expression of CD70 on the PDX tumor cells (~12k/cell), both CARs showed effective tumor control (Supplementary Fig. S7H-I). The memory phenotypes of a class 1 and class 2 following *in vivo* dosing were evaluated and both CARs were predominantly central memory cells (Supplementary Fig. S7J-L). Additionally, rituximab dosed at the time of CAR T administration completely abrogated the CAR T anti-tumor activity in an ACHN xenograft model (Fig. 5H). Based on the above data, the three most active candidates, CARs 3, 17, and 23, were advanced into additional safety assessment.

Tissue Cross-Reactivity study identified minimal off-target binding for CARs 3 and 23

Initial screening of antibodies against a panel of CD70-negative cell lines by flow cytometry identified no off-target binding for CARs 3, 17, and 23 (Sup. Fig. S1B). A tissue cross reactivity (TCR) assay was also performed in which soluble binding domains from CARs 3, 17, and 23 were screened for binding against a panel of 36 normal tissues by immunohistochemistry. Appropriate staining was observed on positive and negative control cell lines (Fig. 6A). All three CARs had membrane staining of leukocytes in lymph nodes and cytoplasmic staining of epithelial cells in the thymus. No additional staining was observed for CAR 3. Staining unique to CAR 17 included cytoplasmic staining in all tissues examined and it was de-prioritized given this broad non-specific staining. CAR 23 displayed cytoplasmic staining of kidney epithelial cells and this was not observed with either of the other CARs, suggestive that the staining is not on-target binding to CD70. A follow-up GLP TCR study was performed with CARs 3 and 23 and findings were similar to those observed previously, with the exception of additional membrane and cytoplasmic staining of resident, migrating, infiltrating, and/or intravascular mononuclear cells (APCs and lymphocytes) in multiple tissues, including lymph node, gut and bronchial-associated lymphoid tissue, and cervix. Given that staining was not widespread and intracellular protein is not accessible to CAR T cells, staining of CAR 3 and CAR 23 was deemed acceptable.

To confirm the CAR 23 staining in normal kidney was limited to the intracellular compartment, normal kidney cells from three donors were evaluated by flow cytometry and subjected to cytotoxicity assays. Normal kidney cells were negative for CD70 staining and did not induce CAR T activation or cytotoxicity (Fig. 6B-F). These data suggest that the CAR 23 staining is of low toxicologic risk.

Minimal adverse findings were seen in a CD70-CD3 bispecific cynomolgus monkey exploratory toxicity study

To further assess potential toxicity liabilities of targeting CD70, a CD70-CD3 bispecific cynomolgus safety study was performed. CAR 23 antibody was reformatted into a bispecific antibody through combination with a CD3 antibody by hinge mutation technology (41). The bispecific antibody displayed a similar affinity for both human and cyno recombinant CD70 protein (5.0 nM vs 7.7 nM). Intravenous injection of the CD70-CD3 bispecific at an initial dose of 30 µg/kg resulted in cytokine release in treated animals (n = 2) (Fig. 7A-B). T cell activation and proliferation (CD69 and ki67 expression; Fig. 7C-D) were also induced, indicating robust activity. Animals displayed signs of cytokine release syndrome (CRS), including emesis, decreased activity, and decreased food consumption, indicating the expected cytokine response to CD3-directed target engagement (42-44). Animals clinically recovered on day 8 and were administered a higher dose of 100µg/kg bispecific to maximize detection of off-target toxicity. Following the second dose, animals showed signs of more severe CRS, including mild tremors, decreased activity and fever, and were euthanized. An extensive panel of normal tissues were collected and subjected to macroscopic and microscopic histopathologic analysis. There were no test article-related macroscopic findings. No microscopic findings were observed in the large majority of tissues examined (Figure 7E). Key findings included decreased cellularity in lymphoid tissues, likely due to elimination of on-target CD70-positive lymphocytes. Additional findings included minimal to mild decreased zymogen granules in salivary glands and the pancreas, an increased myeloid to erythroid ratio that correlated to increased white blood cells, and decreased hemoglobin and platelets in one animal, which may be secondary to CRS and inflammation. Findings were expected based on the expression of CD70 on lymphocytes and the mechanism of action of a CD3 bispecific.

Allogeneic CD70 CAR T cells generated by TALEN® gene-editing at clinical-scale

Success of an allogeneic CAR T cell therapy relies on the ability to produce cells at large scale and treat many patients from a single production run. To verify that CD70 CAR T cells can be generated en masse, a large-scale manufacture process was developed and performed utilizing CAR 23. CAR T cells gene-edited to disrupt the TRAC and CD52 loci were generated from healthy donor PBMCs using an 18-day culture process (Fig. 8A). Cell viability remained high (greater than 95%) throughout the production and CAR T cells expanded more than 30-fold from day 8 to 18, resulting in greater than 4×10^{10} cells at the end of the process (Fig. 8B). The percentage of CD52 and TCR $\alpha\beta$ negative cells was high at the end of production (>60%; Fig. 8C). Remaining TCR-positive cells could contribute to GvHD and were thus purified out successfully using bead-based elimination, resulting in 98.4 % TCR $\alpha\beta$ negativity after purification. The CD70 CAR-positive percentage was ~60% after purification (Fig. 8C). The activity of CD70 CAR 23 T cells produced in the large-scale process was similar to that of CAR T cells generated at small-scale when compared in an *in vitro* cytotoxicity assay (Fig. 8D-E). These data demonstrate the ability to generate highly functional ALLO™ CAR T targeting CD70 at scale and support the use of allogeneic CAR T cells clinically.

DISCUSSION

In this study we found that CD70 has homogenous expression in a high percentage of RCC suggesting it could be an appealing CAR T target. In agreement with previous reports (22) we also found expression on activated T lymphocytes. Such expression might be expected to lead to CAR T cell fratricide, as has been reported for other tumor targets expressed on T cells such as

CD38 and CD7 (45,46). Despite the potential for fratricide, a large number of scFv-based CD70 CARs were successfully transduced and CAR T cells generated.

Extensive *in vitro* analysis of the panel of potential candidate CD70 CAR T cells revealed two general classes based on detection of CD70, one in which CAR T cells displayed increased activation markers, a differentiated memory phenotype, and were highly potent in short-term cytotoxicity assays and the other in which CAR T cells were less activated, less differentiated, and generally displayed inferior cytotoxic activity. Both classes of CARs were capable of masking/protection from fratricide: overexpression of CD70 CARs on ACHN tumor cells was able to protect the cells from lysis by CARs recognizing the same epitope. CD70 was still detected on the surface of the ACHN-CD70 CAR tumor cells with antibodies from another epitope class, suggesting that CD70 is not downregulated on cells upon binding CARs in cis, but rather the CAR is “masking” CD70 and preventing binding. A similar phenomenon has been reported for CD19 and CD5 CARs (47,48). While not followed extensively in our studies, it is possible that CAR T candidates susceptible to fratricide were screened out early in our selection process by low transduction or expansion. Given that both classes of CARs were capable of masking, this phenomenon does not explain the difference between cytotoxic activity of the two classes of CARs.

The binding affinity of Fabs generated from the CARs was very similar between both classes and is likely not the reason for activity difference. A sandwiching assay revealed that the two classes of CARs generally fall into two epitope bins, and this was confirmed by epitope mapping, in which class 1 CARs bound to the membrane distal region of CD70. This region contains the predicted binding epitope for the detection reagent, thus explaining why CD70 is not detectable on class 1 CARs (33). Binding membrane distal epitopes may result in enhanced CAR spacing and sensitivity/potency, thus allowing class 1 CARs to recognize low levels of CD70

expression present on T cells during the CAR T production and leading to activation and differentiation. These CARs were indeed more potent in cytotoxicity assays. Despite generally falling into two classes, unique CARs within each class emerged in certain assays. CAR 23 prevented detection of CD70 by all Fabs when expressed on ACHN cells and this could be due to the specific binding epitope of CAR23 or not only masking, but downregulation of CD70 on the cell surface. CAR 23 ACHN cells were still able to be lysed by CARs of the opposite class, so available CD70 on these cells may be below the detection limit by flow cytometry but still high enough to induce cytotoxicity. The data presented here identify the existence of multiple subsets of CD70 CAR T cells, differing in respect to functionality and highlight the need for evaluating a large number of CAR clones to obtain an optimal candidate.

Despite the potential for CD70 expression on non-transduced cells to drive CAR T exhaustion, CD70 KO did not enhance CAR T expansion, *in vitro* cytotoxicity, or anti-tumor activity of CD70 CAR T cells against a model regarded as having the most physiologically relevant expression. Others have reported enhancements with CD70 KO (49) and we did find enhanced activity of one candidate in a high expression model, suggesting that the benefits of CD70 KO are not universal, but rather scFv and context-dependent. Rituximab off-switch formats were evaluated to mediate CAR T control and in some cases had the added benefit of enhancing CAR T activity, as in the case of CAR 23 in the QR3 format. Given previous published works on the importance of spacers to manipulate CAR T activity (50-52) it could be speculated that for different scFvs, one format of off-switch over another could create the ideal spacing necessary and this may vary by epitope.

To be effective for patients, CAR T cells must possess robust anti-tumor activity, but also demonstrate an appropriate safety profile through extensive toxicological evaluation. A tissue cross-reactivity (TCR) assay was utilized to evaluate binding of the scFvs for three of the most

efficacious CARs against a large panel of normal tissues. The importance of the TCR assay was highlighted by the fact that one of the scFvs, CAR 17, displayed broad cytoplasmic staining in all normal tissues and was removed from further development. In contrast, the remaining two CARs had staining that generally match the reported expression of CD70 in activated lymphocytes and dendritic cells and based on these results CAR 23 was advanced into further toxicological studies.

Toxicologic evaluation of CAR T cells would ideally be done with a cynomolgus CAR T toxicity study. Generation of highly functional cyno CAR T cells and appropriate lymphodepletion to allow for CAR T engraftment makes such studies challenging. However, a cynomolgus CD3 bispecific antibody study is an alternate way to assess the potential for T cell directed killing of on-target/off-target CD70 positive cells and evaluation of internal databases suggested that expression pattern and magnitude of cynomolgus monkey CD70 were similar to that of human CD70. CD70 expression has been reported in activated lymphocytes and DCs, but there are no available reports on toxicity with a highly potent CD70-targeting agent such as CD3 bispecific or CAR T. Here we performed such a study and find that the targeting of CD70 with a CD70-CD3 bispecific antibody in cynomolgus monkeys did not reveal any unexpected findings. Key findings included cytokine release and elimination of mononuclear cells in lymphoid organs, both consistent with the bispecific modality and the reported expression of CD70 on activated lymphocytes. It is expected that treatment with CAR T cells may result in similar decreased cellularity and cytokine release, although the magnitude of cytokine release is difficult to predict. It is possible that the robust activation of T cells by the bispecific (Fig. 7C) may have led to increased CD70 expression on these cells and an increased target burden, potentially exacerbating CRS. Such an effect would not be predicted with allogeneic CAR T cells, in which masking of CD70 by the CAR on the CAR T is expected, and host lymphocytes are suppressed

by lymphodepletion. Doses of CD3 bispecific tested in the study were chosen to produce robust CRS with the expectation that if CRS was observed without other overt toxicity, the risk of either on-target or off target activity of CAR 23 could be considered low. The lack of unexpected findings supports advancement of CAR 23 into clinical studies.

As demonstrated previously (39,40), editing both TRAC and CD52 in CAR T cells was not detrimental to cell function. A clinical-scale process was developed for generation of CD70 AlloCAR T and resulted in the successful manufacturing of >40 billion cells with a 60% CAR+ population and >98% TCR KO. Importantly, CD70 AlloCAR T generated at large-scale displayed similar cytotoxic activity to that of cells from the small-scale process against both CD70 high and low cell lines.

Given the activity, lack of toxicity, and demonstration of manufacturability, these data support clinical evaluation of CD70 allogeneic CAR T cells for the treatment of patients with renal cell carcinoma and this program has advanced into the clinic as ALLO-316.

Acknowledgements

We thank the protein expression and purification group, the flow cytometry group, and the vivarium staff at Allogene Therapeutics, Inc., and Pfizer Inc., for their support. We thank Kevin Lindquist and his group for biosensor expertise and support. We thank Niranjana Nagarajan and Yoon Park for early guidance with the CD70 program. The CD70 CAR target is exclusively licensed from Collectis S.A. and the TALEN® gene-editing technology is pioneered and controlled by Collectis S.A. All work was supported by Allogene Therapeutics

References and Notes

1. Siegel RL, Miller KD, Jemal A. Cancer statistics, 2020. *CA Cancer J Clin* **2020**;70:7-30

2. Bosse D, Ong M. Evolution in upfront treatment strategies for metastatic RCC. *Nat Rev Urol* **2020**;17:73-4
3. Hsieh JJ, Purdue MP, Signoretti S, Swanton C, Albiges L, Schmidinger M, *et al.* Renal cell carcinoma. *Nat Rev Dis Primers* **2017**;3:17009
4. Motzer RJ, Rini BI, McDermott DF, Aren Frontera O, Hammers HJ, Carducci MA, *et al.* Nivolumab plus ipilimumab versus sunitinib in first-line treatment for advanced renal cell carcinoma: extended follow-up of efficacy and safety results from a randomised, controlled, phase 3 trial. *Lancet Oncol* **2019**;20:1370-85
5. Rini BI, Plimack ER, Stus V, Gafanov R, Hawkins R, Nosov D, *et al.* Pembrolizumab plus Axitinib versus Sunitinib for Advanced Renal-Cell Carcinoma. *N Engl J Med* **2019**;380:1116-27
6. Motzer R, Alekseev B, Rha SY, Porta C, Eto M, Powles T, *et al.* Lenvatinib plus Pembrolizumab or Everolimus for Advanced Renal Cell Carcinoma. *N Engl J Med* **2021**;384:1289-300
7. Chevrier S, Levine JH, Zanotelli VRT, Silina K, Schulz D, Bacac M, *et al.* An Immune Atlas of Clear Cell Renal Cell Carcinoma. *Cell* **2017**;169:736-49 e18
8. Boyiadzis MM, Dhodapkar MV, Brentjens RJ, Kochenderfer JN, Neelapu SS, Maus MV, *et al.* Chimeric antigen receptor (CAR) T therapies for the treatment of hematologic malignancies: clinical perspective and significance. *Journal for immunotherapy of cancer* **2018**;6:137
9. Mikkilineni L, Kochenderfer JN. CAR T cell therapies for patients with multiple myeloma. *Nature reviews Clinical oncology* **2020**
10. Mullard A. FDA approves fourth CAR-T cell therapy. *Nature reviews Drug discovery* **2021**;20:166
11. Kansagra A, Farnia S, Majhail N. Expanding Access to Chimeric Antigen Receptor T-Cell Therapies: Challenges and Opportunities. *Am Soc Clin Oncol Educ Book* **2020**;40:1-8
12. Srivastava S, Riddell SR. Chimeric Antigen Receptor T Cell Therapy: Challenges to Bench-to-Bedside Efficacy. *Journal of immunology* **2018**;200:459-68
13. Schuster SJ, Bishop MR, Tam CS, Waller EK, Borchmann P, McGuirk JP, *et al.* Tisagenlecleucel in Adult Relapsed or Refractory Diffuse Large B-Cell Lymphoma. *N Engl J Med* **2019**;380:45-56
14. Singh N, Perazzelli J, Grupp SA, Barrett DM. Early memory phenotypes drive T cell proliferation in patients with pediatric malignancies. *Sci Transl Med* **2016**;8:320ra3
15. Fraietta JA, Lacey SF, Orlando EJ, Pruteanu-Malinici I, Gohil M, Lundh S, *et al.* Determinants of response and resistance to CD19 chimeric antigen receptor (CAR) T cell therapy of chronic lymphocytic leukemia. *Nature medicine* **2018**;24:563-71
16. Ghassemi S, Nunez-Cruz S, O'Connor RS, Fraietta JA, Patel PR, Scholler J, *et al.* Reducing Ex Vivo Culture Improves the Antileukemic Activity of Chimeric Antigen Receptor (CAR) T Cells. *Cancer Immunol Res* **2018**;6:1100-9
17. Hoffmann JM, Schubert ML, Wang L, Huckelhoven A, Sellner L, Stock S, *et al.* Differences in Expansion Potential of Naive Chimeric Antigen Receptor T Cells from Healthy Donors and Untreated Chronic Lymphocytic Leukemia Patients. *Front Immunol* **2017**;8:1956
18. Itzhaki O, Jacoby E, Nissani A, Levi M, Nagler A, Kubi A, *et al.* Head-to-head comparison of in-house produced CD19 CAR-T cell in ALL and NHL patients. *Journal for immunotherapy of cancer* **2020**;8

19. Magalhaes I, Kalland I, Kochenderfer JN, Osterborg A, Uhlin M, Mattsson J. CD19 Chimeric Antigen Receptor T Cells From Patients With Chronic Lymphocytic Leukemia Display an Elevated IFN-gamma Production Profile. *J Immunother* **2018**;41:73-83
20. Petersen CT, Hassan M, Morris AB, Jeffery J, Lee K, Jagirdar N, *et al.* Improving T-cell expansion and function for adoptive T-cell therapy using ex vivo treatment with PI3Kdelta inhibitors and VIP antagonists. *Blood Adv* **2018**;2:210-23
21. Depil S, Duchateau P, Grupp SA, Mufti G, Poirot L. 'Off-the-shelf' allogeneic CAR T cells: development and challenges. *Nature reviews Drug discovery* **2020**;19:185-99
22. Borst J, Hendriks J, Xiao Y. CD27 and CD70 in T cell and B cell activation. *Curr Opin Immunol* **2005**;17:275-81
23. Hendriks J, Xiao Y, Rossen JW, van der Sluijs KF, Sugamura K, Ishii N, *et al.* During viral infection of the respiratory tract, CD27, 4-1BB, and OX40 collectively determine formation of CD8+ memory T cells and their capacity for secondary expansion. *Journal of immunology* **2005**;175:1665-76
24. Keller AM, Groothuis TA, Veraar EA, Marsman M, Maillette de Buy Wenniger L, Janssen H, *et al.* Costimulatory ligand CD70 is delivered to the immunological synapse by shared intracellular trafficking with MHC class II molecules. *Proceedings of the National Academy of Sciences of the United States of America* **2007**;104:5989-94
25. Denoed J, Moser M. Role of CD27/CD70 pathway of activation in immunity and tolerance. *J Leukoc Biol* **2011**;89:195-203
26. Nolte MA, van Olfen RW, van Gisbergen KP, van Lier RA. Timing and tuning of CD27-CD70 interactions: the impact of signal strength in setting the balance between adaptive responses and immunopathology. *Immunol Rev* **2009**;229:216-31
27. Grewal IS. CD70 as a therapeutic target in human malignancies. *Expert Opin Ther Targets* **2008**;12:341-51
28. Law CL, Gordon KA, Toki BE, Yamane AK, Hering MA, Cerveny CG, *et al.* Lymphocyte activation antigen CD70 expressed by renal cell carcinoma is a potential therapeutic target for anti-CD70 antibody-drug conjugates. *Cancer Res* **2006**;66:2328-37
29. Diegmann J, Junker K, Loncarevic IF, Michel S, Schimmel B, von Eggeling F. Immune escape for renal cell carcinoma: CD70 mediates apoptosis in lymphocytes. *Neoplasia* **2006**;8:933-8
30. Jin L, Ge H, Long Y, Yang C, Chang YE, Mu L, *et al.* CD70, a novel target of CAR T-cell therapy for gliomas. *Neuro Oncol* **2018**;20:55-65
31. Shaffer DR, Savoldo B, Yi Z, Chow KK, Kakarla S, Spencer DM, *et al.* T cells redirected against CD70 for the immunotherapy of CD70-positive malignancies. *Blood* **2011**;117:4304-14
32. Wang QJ, Yu Z, Hanada KI, Patel K, Kleiner D, Restifo NP, *et al.* Preclinical Evaluation of Chimeric Antigen Receptors Targeting CD70-Expressing Cancers. *Clinical cancer research : an official journal of the American Association for Cancer Research* **2017**;23:2267-76
33. Silence K, Dreier T, Moshir M, Ulrichs P, Gabriels SM, Saunders M, *et al.* ARGX-110, a highly potent antibody targeting CD70, eliminates tumors via both enhanced ADCC and immune checkpoint blockade. *mAbs* **2014**;6:523-32
34. Zhai W, Glanville J, Fuhrmann M, Mei L, Ni I, Sundar PD, *et al.* Synthetic antibodies designed on natural sequence landscapes. *Journal of molecular biology* **2011**;412:55-71
35. Van Blarcom T, Lindquist K, Melton Z, Cheung WL, Wagstrom C, McDonough D, *et al.* Productive common light chain libraries yield diverse panels of high affinity bispecific antibodies. *mAbs* **2018**;10:256-68

36. Long AH, Haso WM, Shern JF, Wanhainen KM, Murgai M, Ingaramo M, *et al.* 4-1BB costimulation ameliorates T cell exhaustion induced by tonic signaling of chimeric antigen receptors. *Nature medicine* **2015**;21:581-90
37. Zhou X, Di Stasi A, Brenner MK. iCaspace 9 Suicide Gene System. *Methods in molecular biology* **2015**;1317:87-105
38. Valton J, Guyot V, Boldajipour B, Sommer C, Pertel T, Juillerat A, *et al.* A Versatile Safeguard for Chimeric Antigen Receptor T-Cell Immunotherapies. *Scientific reports* **2018**;8:8972
39. Sommer C, Cheng HY, Nguyen D, Dettling D, Yeung YA, Sutton J, *et al.* Allogeneic FLT3 CAR T Cells with an Off-Switch Exhibit Potent Activity against AML and Can Be Depleted to Expedite Bone Marrow Recovery. *Mol Ther* **2020**;28:2237-51
40. Sommer C, Boldajipour B, Kuo TC, Bentley T, Sutton J, Chen A, *et al.* Preclinical Evaluation of Allogeneic CAR T Cells Targeting BCMA for the Treatment of Multiple Myeloma. *Mol Ther* **2019**;27:1126-38
41. Strop P, Ho WH, Boustany LM, Abdiche YN, Lindquist KC, Farias SE, *et al.* Generating bispecific human IgG1 and IgG2 antibodies from any antibody pair. *Journal of molecular biology* **2012**;420:204-19
42. Engelberts PJ, Hiemstra IH, de Jong B, Schuurhuis DH, Meesters J, Beltran Hernandez I, *et al.* DuoBody-CD3xCD20 induces potent T-cell-mediated killing of malignant B cells in preclinical models and provides opportunities for subcutaneous dosing. *EBioMedicine* **2020**;52:102625
43. Shimabukuro-Vornhagen A, Godel P, Subklewe M, Stemmler HJ, Schlosser HA, Schlaak M, *et al.* Cytokine release syndrome. *Journal for immunotherapy of cancer* **2018**;6:56
44. Staflin K, Zuch de Zafra CL, Schutt LK, Clark V, Zhong F, Hristopoulos M, *et al.* Target arm affinities determine preclinical efficacy and safety of anti-HER2/CD3 bispecific antibody. *JCI Insight* **2020**;5
45. Gao Z, Tong C, Wang Y, Chen D, Wu Z, Han W. Blocking CD38-driven fratricide among T cells enables effective antitumor activity by CD38-specific chimeric antigen receptor T cells. *J Genet Genomics* **2019**;46:367-77
46. Gomes-Silva D, Atilla E, Atilla PA, Mo F, Tashiro H, Srinivasan M, *et al.* CD7 CAR T Cells for the Therapy of Acute Myeloid Leukemia. *Mol Ther* **2019**;27:272-80
47. Mamonkin M, Rouce RH, Tashiro H, Brenner MK. A T-cell-directed chimeric antigen receptor for the selective treatment of T-cell malignancies. *Blood* **2015**;126:983-92
48. Ruella M, Xu J, Barrett DM, Fraietta JA, Reich TJ, Ambrose DE, *et al.* Induction of resistance to chimeric antigen receptor T cell therapy by transduction of a single leukemic B cell. *Nature medicine* **2018**;24:1499-503
49. Dequeant M, Sagert J, Kalaitzidis D, Keerthipati P, Terrett J. CD70 knockout: A novel approach to augment CAR-T function. *AACR 2021* **2021**
50. Guest RD, Hawkins RE, Kirillova N, Cheadle EJ, Arnold J, O'Neill A, *et al.* The role of extracellular spacer regions in the optimal design of chimeric immune receptors: evaluation of four different scFvs and antigens. *J Immunother* **2005**;28:203-11
51. Hudecek M, Lupo-Stanghellini MT, Kosasih PL, Sommermeyer D, Jensen MC, Rader C, *et al.* Receptor affinity and extracellular domain modifications affect tumor recognition by ROR1-specific chimeric antigen receptor T cells. *Clinical cancer research : an official journal of the American Association for Cancer Research* **2013**;19:3153-64
52. James SE, Greenberg PD, Jensen MC, Lin Y, Wang J, Till BG, *et al.* Antigen sensitivity of CD22-specific chimeric TCR is modulated by target epitope distance from the cell membrane. *Journal of immunology* **2008**;180:7028-38

Figure Legends

Figure 1. CD70 is expressed in renal cell carcinoma cell lines and tumors, with limited expression in normal tissue. RCC renal cell carcinoma, Kdn kidney, Bld bladder, Adr adrenal, Brn brain, Cln colon, Hrt heart, Itn intestine, Lvr liver, Lng lung, Nrv nerve, Pnc pancreas, Skn skin, Spl spleen, Stm stomach. **A**, mRNA expression of *CD70* in malignant and normal tissues as seen in TCGA and GTEx RNAseq data sets; TPM, transcripts per kilobase million. **B**, mRNA expression in RCC samples (red dots, n = 534) and RCC tumor cell lines (black dots, n = 20) according to TCGA and CCLE RNASeq data sets **C**, Tissue microarrays of patient samples for clear cell (n = 227), papillary (n = 12), sarcomatoid (n = 8), chromophobe (n = 7), and transitional RCC were immunostained for CD70 and scored by a pathologist. **D**, Representative images are shown for ccRCC with CD70 (brown) and hematoxylin (blue) staining. Scale bar, 100µm. **E**, Cell surface expression of CD70 in RCC primary patient samples and cell lines as measured by flow cytometry. **F**, CD70 receptor quantification in primary patient samples (n = 10); black bar represents median of 7k; ABC, antibody binding capacity **G**, CD70 cell-surface expression on non-activated and activated T cells measured by flow cytometry. T cells were activated for 6 days.

Figure 2. CD70 CAR T *in vitro* characterization reveals different classes of CARs and identifies optimal clones. **A**, CARs were screened for auto-activation using a Jurkat cell assay. Activation (CD69 expression) was characterized as autoactivation if occurring even with CD70 KO. **B**, Primary T cells were transduced with CD70 CARs (detected on day 14) as determined by BFP co-expression (x-axis). Four representative CARs are shown. **C**, CD70 detection on CAR T cells was evaluated by flow cytometry. **D**, CAR T cell memory phenotypes were determined by expression of CD62L and CD45RO. **E**, CAR T cell activation (4-1BB⁺, CD25⁺) was measured by flow cytometry. Examples of activated (CARs 17 and 23) or less activated (CARs 1 and 24) are shown. **F**, CD70 CAR T cells effectively lysed target cells *in vitro*. CAR T cells and luciferase-labeled CD70-high (786-O), CD70-low (ACHN), and CD70-very low (REH) were co-cultured for 72 hours, followed by ONE-Glo luminescent measurement to assess target cell viability. **G**, Comparison of the relationship between cytolytic activity and detection of CD70 of CAR T cells, in which CARs with minimal CD70 detection by clone 41D12 were generally more cytolytic. CD70 expression data is from panel C. Cytotoxicity data is from panel F using the 1:3 E:T ratio for the CD70-high targets (786-O) and the 1:3 ratio for the CD70-low targets (REH). **H**, Activity of CD70 CAR T cells in a long-term killing assay. CAR T cells and target cells were co-cultured at E:T ratios of 3:1, 10:1, and 1:5 for 786-O, ACHN, and REH cells, respectively. For cytotoxicity assays, four CARs are highlighted as examples and all other CARs are shown in gray. Data are shown for one representative biological replicate with three technical replicates. Data are shown as mean ± SEM for one CAR T cell donor against triplicate tumor samples. Similar trends were observed when repeated with a second donor.

Figure 3. CD70 CAR expression protects CD70⁺ cells from fratricide. **A**, CD70 CAR expression may lead to recognition and elimination of neighboring T cells (fratricide) or alternatively may

bind CD70 in cis and mask detection, thus preventing fratricide. **B**, Class 1 CARs do not show detectable CD70 expression even when fratricide is not possible. Jurkat cells were transduced with CD70 CARs and evaluated for CD70 expression by flow cytometry with clone 41D12 (class 1-like). **C**, Representative CAR and CD70 detection on class 1 (CAR 3) and class 2 (CAR 1) CAR Jurkat cells. **D**, CD70 trimer is shown as solid surface with one monomer colored in wheat. The epitope residues identified for class 1 and class 2 CARs are colored in red and green, respectively. **E**, CD70 ACHN cells can only be detected by Fabs from the alternate class. Cells were engineered to overexpress class 1 or class 2 CARs and stained for CD70 with either class 1 or class 2 Fabs. **F**, ACHN cells overexpressing class 1 CARs can be killed by class 2 but not class 1 CARs. The exception to this was CAR 24, which cannot kill class 1 CAR expressing cells. Data are shown as mean \pm SEM for one CAR T cell donor against triplicate tumor samples. **G**, ACHN cells overexpressing class 2 CARs can be killed by class 1 but not class 2 CARs. The exception to this was CAR 24 (blue), which was only protective against itself.

Figure 4. CD70 KO does not improve the activity of CAR T cells against CD70-low tumor cells *in vitro* and *in vivo*. **A**, CD70 TALEN® electroporation resulted in a >95% reduction in CD70 expression on NTD cells relative to the mock control. CD70 CAR T cells and non-transduced (NTD) control T cells were electroporated with CD70 TALEN® and analyzed by flow cytometry at the end of CAR production. **B**, CD70 KO and wild type cells were equally efficient at killing ACHN cells in a short-term cytotoxicity assay. Luciferase-labeled ACHN target cells were co-cultured with CAR T or NTD cells, either with or without CD70 KO, for 72 hours at the indicated E:T ratios and ACHN viability determined by ONE-Glo luminescent measurement. **C**, CD70 CAR 23 demonstrated dose-dependent anti-tumor activity in a CD70-high 786-O xenograft model. NSG mice were engrafted subcutaneously (SC) with 786-O cells and treated

with a single intravenous (IV) dose of 1×10^6 , 3×10^6 , and 5×10^6 CAR⁺ cells. Tumor burden was monitored by caliper measurement twice weekly (n=10). **D**, CD70 CAR 23 demonstrated dose-dependent anti-tumor activity in a CD70-low ACHN xenograft model. Mice were administered ACHN cells IV and treated with a single IV dose of 1×10^6 , 3×10^6 , and 5×10^6 CAR⁺ cells 14 days later (n=5). Luminescent imaging was used to measure tumor flux twice weekly. **E**, CD70 CAR T clones with or without CD70 KO demonstrated anti-tumor activity in a 786-O RCC xenograft model. Study was performed as described in C. Mice were dosed at 3×10^6 CAR⁺ cells, (n=10). **F**, CD70 CAR T clones with or without CD70 KO demonstrated equivalent anti-tumor activity in an ACHN metastatic RCC xenograft model. Study was performed as described in D. Mice were dosed at 3×10^6 CAR⁺ cells, (n=5). Data are presented as mean \pm SEM. Statistics represent RMANOVA with Tukey's multiple comparison test, each group compared to corresponding NTD control (**** p \leq 0.0001, ** p \leq 0.01, * p \leq 0.05, ns p $>$ 0.05).

Figure 5. CD70 CAR T with rituximab-based off-switches are active *in vitro* and *in vivo*.

A, CD70 CAR designs with rituximab-based off-switch formats. Rituximab mimotopes were placed either N or C-terminal to the scFv. **B**, Pan T cells were transduced with CAR constructs. Rituximab-positivity on day 14 of production ranged from 34-91%, as determined by flow cytometry with rituximab. **C**, CD70 CAR T cells with off-switches all effectively lysed luciferase-labeled 786-O cells *in vitro*. CAR T and tumor cells were co-cultured for 72 hours, followed by ONE-Glo luminescent measurement to assess target cell viability. 786-O target cell viability at the 3:1 E:T ratio was plotted **D**, and the rituximab format with the greatest cytotoxic activity for each CAR (red arrows) was moved into *in vivo* evaluation. **E**, CD70 CAR 23 QR3 displayed enhanced anti-tumor activity in a CD70-high 786-O xenograft model. NSG mice were engrafted SC with 786-O cells and dosed with 3×10^6 CAR⁺ cells. Tumor burden was monitored

by caliper measurement twice weekly (n=10). **F**, CD70 CAR T clones with rituximab off-switches demonstrated anti-tumor activity in the 786-O RCC xenograft model. Mice were dosed at 5×10^6 CAR⁺ cells per animal, (n = 6-8). Tumor burden was determined by caliper measurement twice weekly. **G**, CD70 CAR T clones with rituximab off-switches demonstrated anti-tumor activity in the CD70-low ACHN RCC metastasis model. Luciferase-labeled tumor cells were inoculated IV and mice were dosed with 5×10^6 CAR⁺ (n = 5). Tumor burden was monitored by luminescent imaging twice weekly. **H**, Dosing of rituximab reduces CAR T antitumor activity *in vivo*. Tumor-bearing animals were dosed with 3×10^6 NTD or CAR 23-QR3 cells and subsequently administered rituximab or PBS control (n=10). Rituximab was dosed intraperitoneally at 10 mg/kg for 5 consecutive days beginning on the day of CAR T administration. Data are presented as mean \pm SEM. Statistics represent RMANOVA with Tukey's multiple comparison test, each group compared to corresponding NTD control (**** $p \leq 0.0001$, ** $p \leq 0.01$).

Figure 6. Tissue Cross-Reactivity study identified minimal off-target binding for CARs 3 and 23. The scFv binding domains of CARs 3, 17, and 23 were fused to a human IgG2 Fc fragment and assayed using immunohistochemistry (IHC) against a panel of 36 human tissues to evaluate binding **A**. Results are shown for staining at 2 μ g/mL. CD70-positive and negative cell pellets were utilized as controls. Staining was scored by a board-certified pathologist on both intensity and frequency. Scoring is shown for control cell pellets and for tissues in which positive staining with either CARs 3 or 23 was observed. **B**, No CD70 expression was observed on primary kidney samples from three donors. Kidney samples were divided into cortex and medulla, dissociated, and evaluated by flow cytometry with soluble CAR 23 scFv-Fc protein or isotype control. Co-incubation of dissociated kidney cortex **C**, or medulla **D**, did not activate CAR 23 T

cells as compared to the CAR T alone as determined by flow cytometry for CD69 expression. Cells were incubated at a 1:1 E:T ratio for 24 hours. CAR 23 T cells did not kill dissociated kidney medulla **E**, or cortex **F**, cells in a 24-hour cytotoxicity assay.

Figure 7. No overt toxicity was observed in a cynomolgus monkey CD70-CD3 bispecific study. CAR 23 was reformatted as a CD70-CD3 bispecific IgG and utilized in a cynomolgus exploratory toxicity study. The bispecific was administered IV and animals (n=2) were dosed twice (30µg/kg on day 1, 100µg/kg on day 8). The CD70 bispecific was highly active and resulted in elevated IL6 **A**, and IL10 **B**, compared to vehicle treated animals. Day 2 timepoint shown is 24 hours post dosing. T cell activation indicated by CD69 (**C**) and proliferation indicated by Ki67 **D**, were observed by flow cytometry in the CD70 bispecific groups but not control animals. An extensive panel of normal tissues were collected on day 8 and evaluated for macroscopic and microscopic findings by a board-certified pathologist. No macroscopic findings were observed. Microscopic findings **E**, were scored as grade 1 (minimal), grade 2 (mild), grade 4 (marked), or “no findings”. No findings were observed in the vehicle treated control group.

Figure 8. Allogeneic CD70 CAR T cells can be generated by TALEN® gene-editing and manufactured in a clinical-scale process. **A**, CD70 CAR T cells were successfully manufactured in a large-scale process. PBMCs were activated on day 2, transduced with CAR on day 4, electroporated with TALEN® mRNA for TRAC and CD52 on day 6, and expanded until day 18 **B**, The process yielded greater than 4×10^{10} total cells with high viability over 18 days. **C**, Cells produced in the large-scale process described in (A) were analyzed for CAR expression, CD52 KO, and TRAC KO by flow cytometry. CD70 CAR⁺ percentage, CD52 KO, and TCR KO were 47%, 63%, and 78% respectively prior to TCRαβ⁻ purification and 63%, 71%, and 98% after

TCR $\alpha\beta$ ⁻ purification. No marked difference in cytotoxic activity was observed between large- and small-scale CAR production processes as demonstrated against ACHN **D**, and 786-O **E**, *in vitro*. CAR T and target cells were incubated at the indicated E:T ratios for 72 hours, followed by ONE-Glo luminescent measurement of target cell viability. Each condition was run in triplicate. Results shown as mean \pm SEM.

Fig. 1

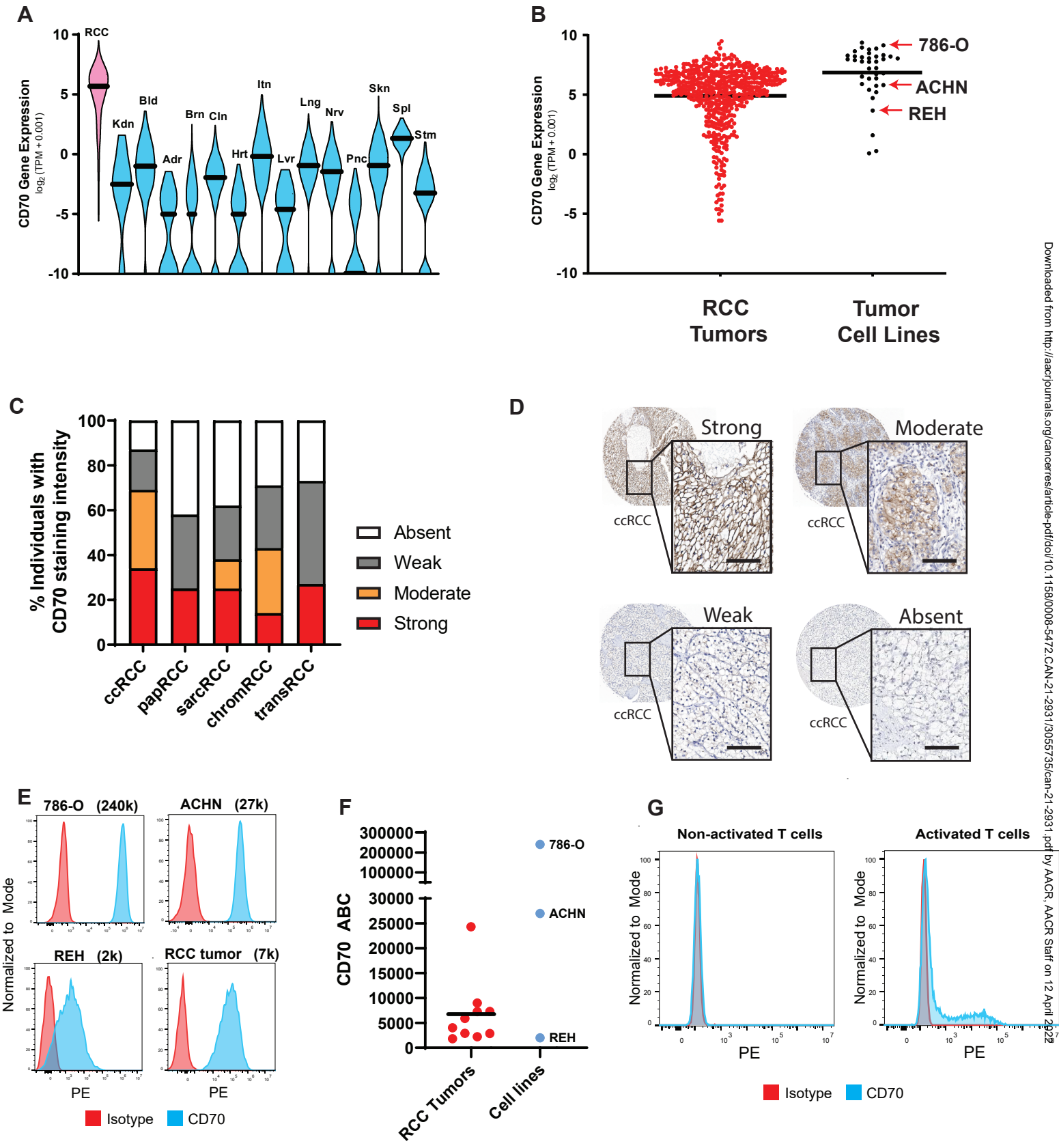


Fig. 2

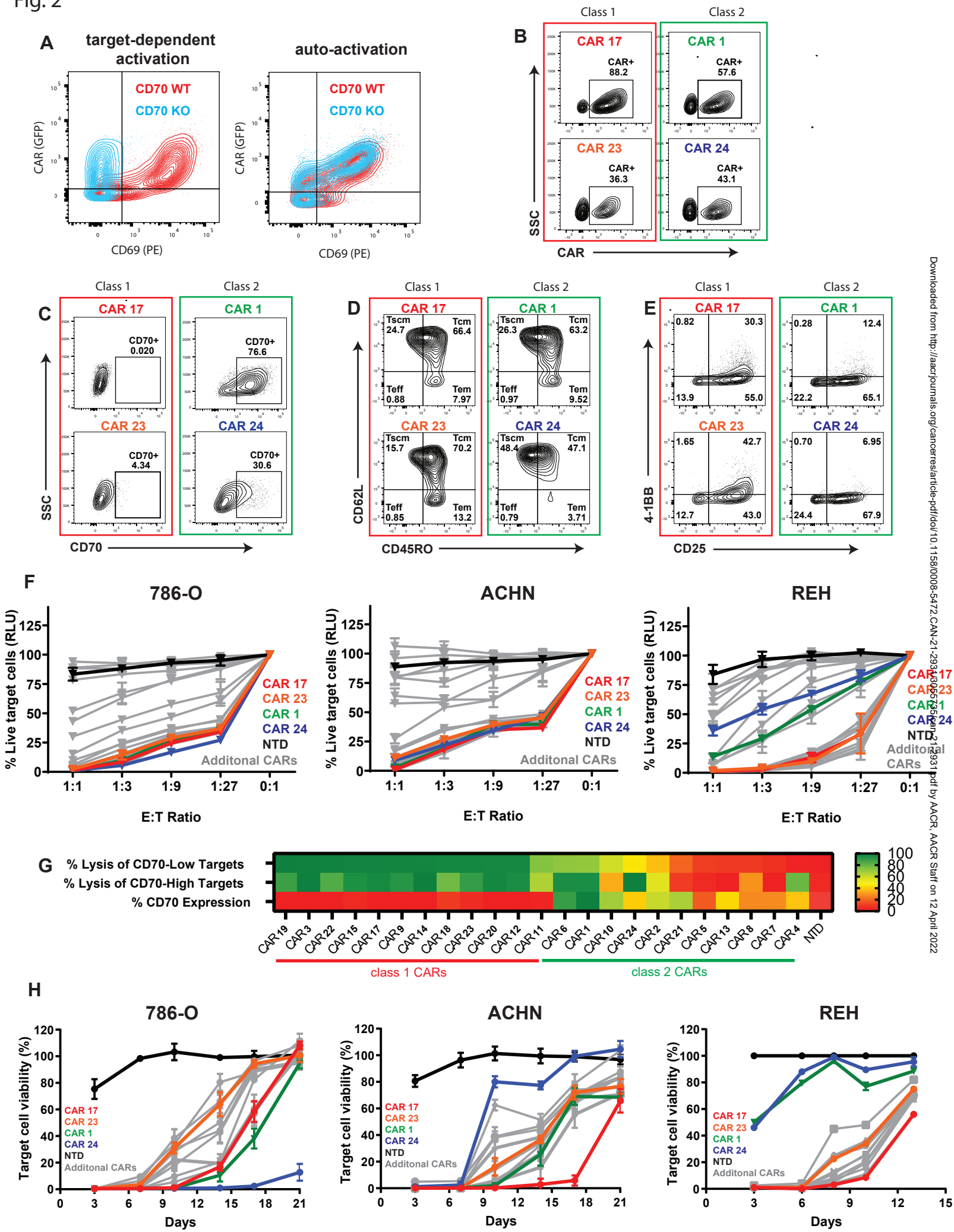


Fig. 3

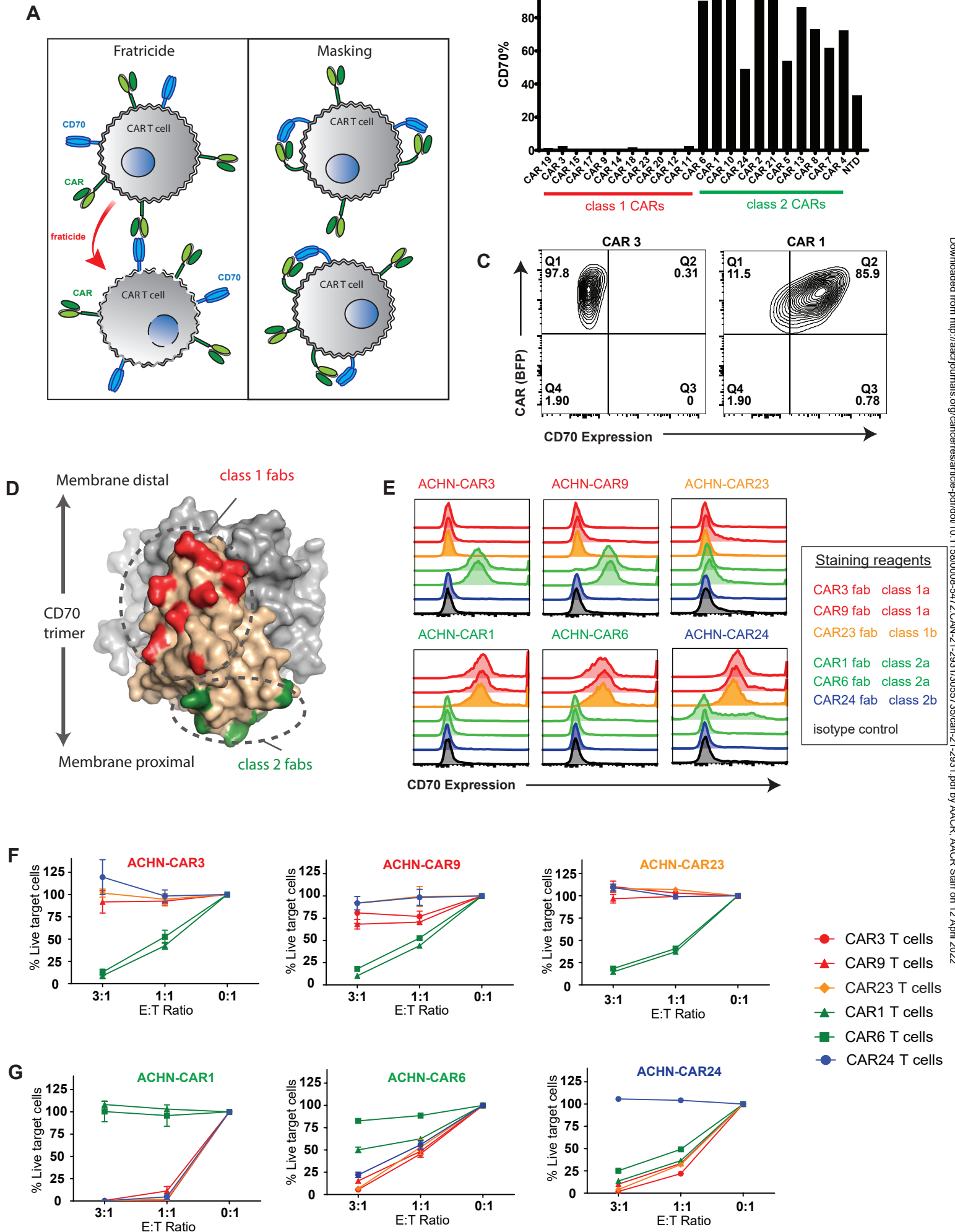
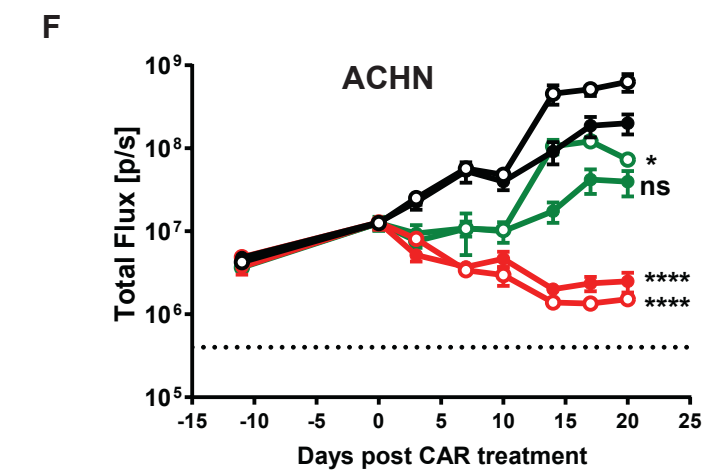
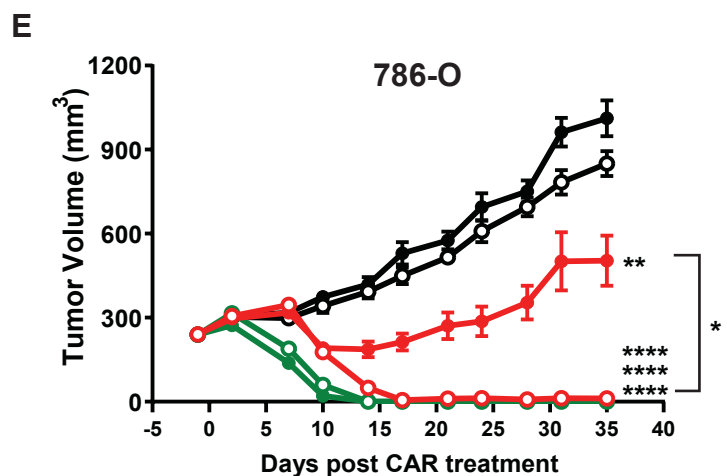
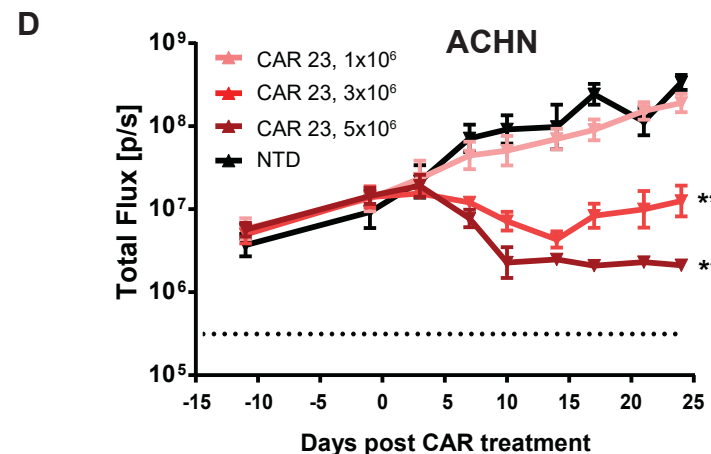
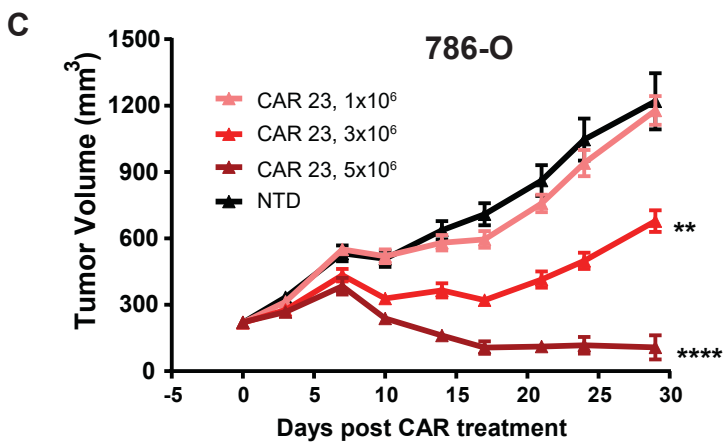
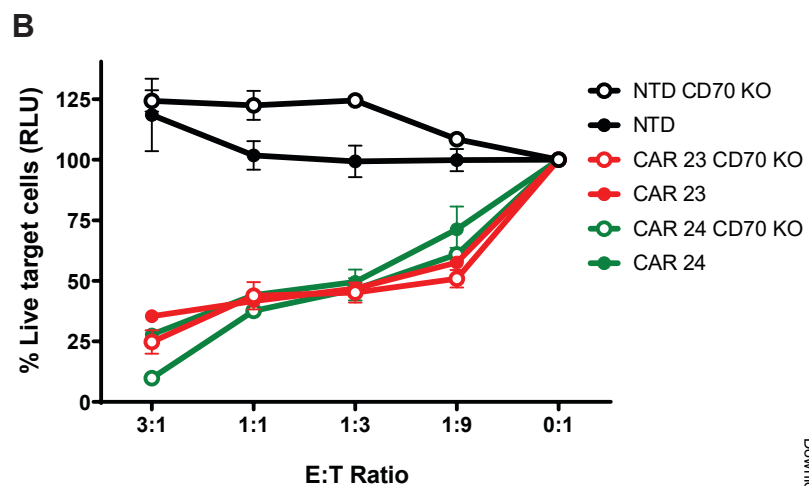
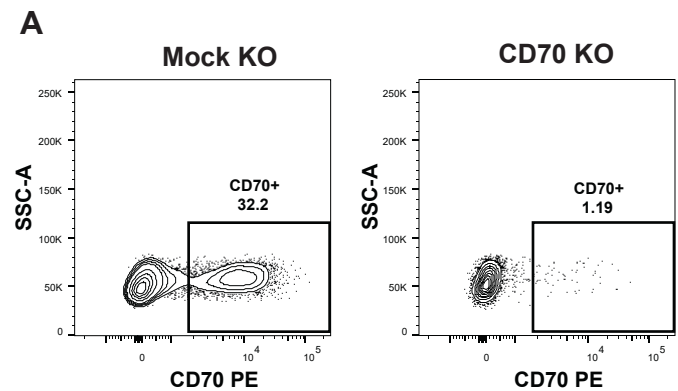


Fig. 4



● NTD ● CAR 23 ● CAR 24
 ○ NTD CD70 KO ○ CAR 23 CD70 KO ○ CAR 24 CD70 KO

Fig. 5

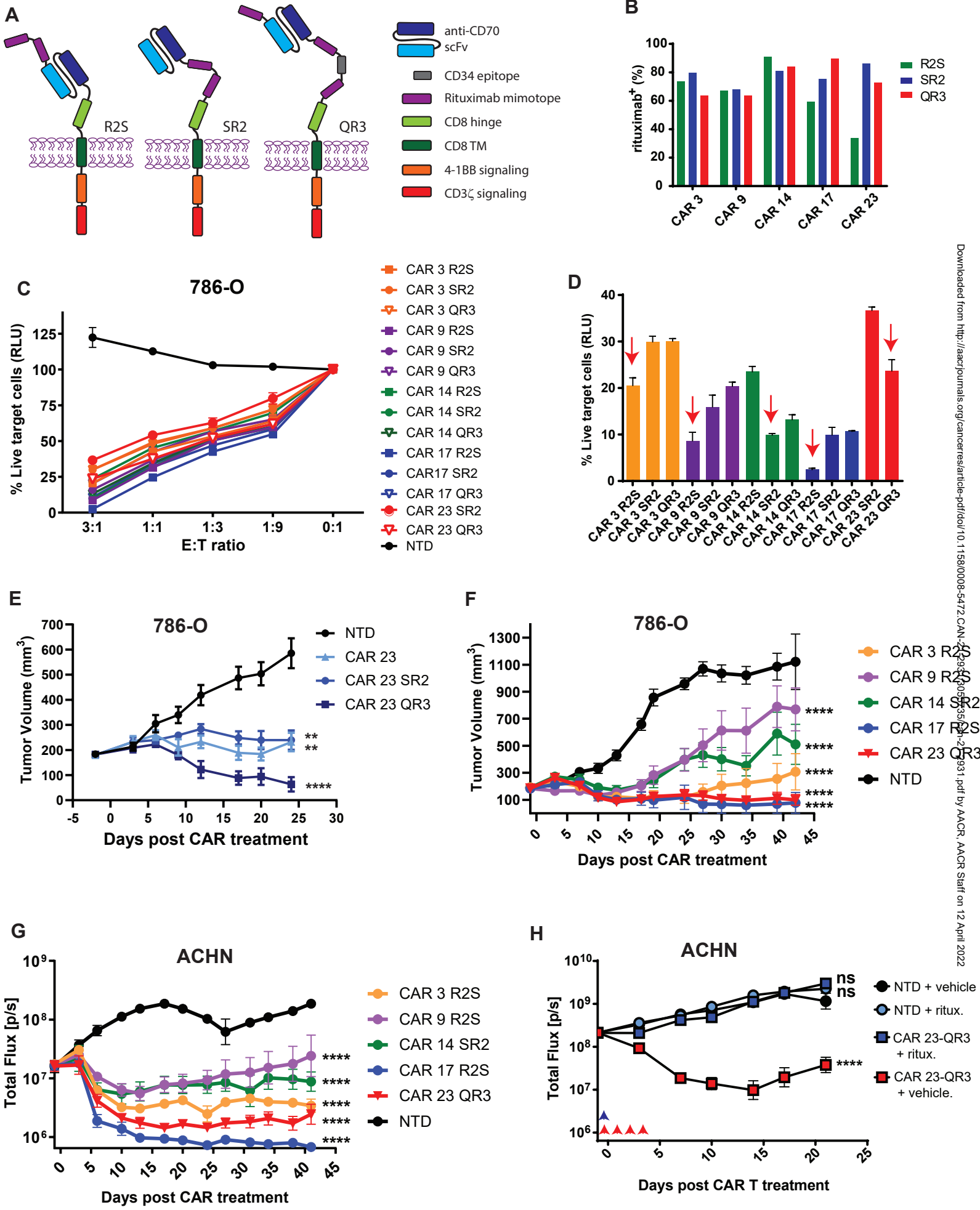


Fig. 6

A

Cell line/Tissue	CAR3	CAR17	CAR23
ACHN (CD70 ⁺)	1-3+, freq, M	2-3+, freq, M	1-3+, freq, M
Raji (CD70 ⁺)	3-4+, freq, M	3-4+, freq, M	3-4+, freq, M
786-O (CD70 ⁺)	2-4+, freq, M	2-4+, freq, M	2-4+, freq, M
293T (CD70 ⁻)	nega ve	nega ve	nega ve
786-O CD70 KO (CD70 ⁻)	nega ve	nega ve	nega ve
Kidney, epithelial tubules	nega ve	nega ve	2-4+, occas, C
Lymph Node (leukocytes)	1-3+, rare, M	1-3+, occas, M	1-3+, rare to occas, M
Spleen (leukocytes)	nega ve	1-3+, freq, M	nega ve
Thymus (epithelial-re cular cells)	2-3+, occas, C	2-3+, freq, C	2-3+, occas, C
Thymus (leukocytes)	nega ve	1-3+, occas, M	nega ve

1+ = weak, 2+ = moderate, 3+ = strong, 4+ = intense, negative (0%), rare (>1-5%), rare to occas (>5-25%), occas = occasional (>25-50%)
freq = frequent (75-100%), M = membrane staining, C = cytoplasmic staining

CAR17 displayed 1-3, freq cytoplasmic staining in all tissues evaluated

CAR3 and CAR 23 displayed no staining in adrenal, bladder, blood cells, blood vessels, bone marrow, brain - cerebellum, brain - cerebral, breast, colon, eye, fallopian tube, GI tract - esophagus, GI tract - small intestine, GI tract - stomach, heart, liver, lung, ovary, pancreas, parathyroid, peripheral nerve, pituitary, placenta, prostate, salivary gland, skin, spinal cord, striated muscle, testis, thyroid, tonsil, ureter, uterus - cervix, uterus - endometrium,

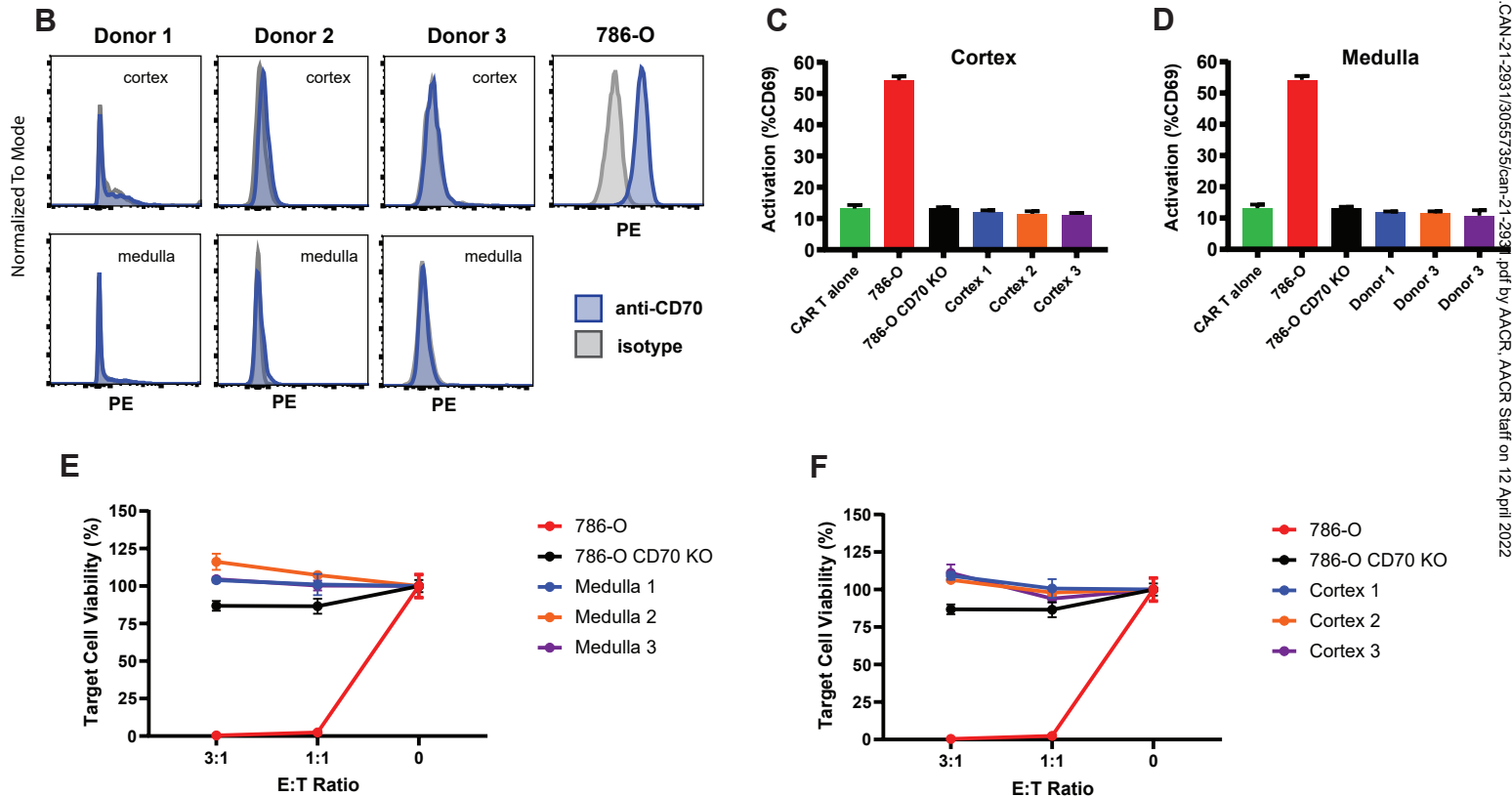


Fig. 8

